Neuron
Article

# Inferotemporal Cortex Subserves Three-Dimensional Structure Categorization

Bram-Ernst Verhoef,[1] Rufin Vogels,[1] and Peter Janssen[1,*]
[1]Laboratorium voor Neuro- en Psychofysiologie, Campus Gasthuisberg, O&N2, Herestraat 49, Bus 1021, BE 3000 Leuven, Belgium
*Correspondence: peter.janssen@med.kuleuven.be
DOI 10.1016/j.neuron.2011.10.031

## SUMMARY

**We perceive real-world objects as three-dimensional (3D), yet it is unknown which brain area underlies our ability to perceive objects in this way. The macaque inferotemporal (IT) cortex contains neurons that respond selectively to 3D structures defined by binocular disparity. To examine the causal role of IT in the categorization of 3D structures, we electrically stimulated clusters of IT neurons with a similar 3D-structure preference while monkeys performed a 3D-structure categorization task. Microstimulation of 3D-structure-selective IT clusters caused monkeys to choose the preferred structure of the 3D-structure-selective neurons considerably more often. Microstimulation in IT also accelerated the monkeys' choice for the preferred structure, while delaying choices corresponding to the nonpreferred structure of a given site. These findings reveal that 3D-structure-selective neurons in IT contribute to the categorization of 3D objects.**

## INTRODUCTION

We perceive a world filled with three-dimensional (3D) objects even though 3D objects are projected onto a two-dimensional (2D) retinal image. Hence, the perception of 3D structures needs to be constructed by the brain. Yet, how and where 3D-structure perception arises from the activity of neurons within the brain remains an unanswered question.

One candidate for an area that could subserve 3D-structure perception is the inferotemporal (IT) cortex. IT contains shape-selective neurons whose responses are typically tolerant to various image transformations such as changes in size, position (in depth), or defining cue (Ito et al., 1995; Janssen et al., 2000; Sáry et al., 1993; Schwartz et al., 1983; Vogels, 1999). These properties make it likely that IT neurons underlie object recognition and categorization (Logothetis and Sheinberg, 1996; Tanaka, 1996). Nonetheless, it has thus far proved difficult to unequivocally relate IT neurons having particular shape preferences to a given perceptual behavior that relies on the information encoded by those neurons. Moreover, although the representation of 3D structure is intrinsically linked to the representation of objects, the third shape dimension has hitherto received relatively little attention.

The 3D structure of objects can be signaled by a variety of depth cues (Howard and Rogers, 1995). A particularly powerful way of computing 3D structure relies on stereo-vision and the binocular disparities originating from the slightly different projections of the world onto the retina of each eye. Neurons that respond selectively to binocular disparity have been observed throughout the macaque brain (see Anzai and DeAngelis, 2010; Parker, 2007, for reviews). Area V1 is the first stage in the visual hierarchy where neurons show disparity selectivity but several ventral, dorsal, and even frontal areas process disparity as well (Ferraina et al., 2000; Janssen et al., 1999; Joly et al., 2009; Nienborg and Cumming, 2006; Srivastava et al., 2009; Thomas et al., 2002; Tsutsui et al., 2001; Umeda et al., 2007; Yamane et al., 2008). The ubiquity of disparity-processing neurons in the brain suggests the importance of disparity for both visual perception and visually guided movements. However, research thus far has focused mainly on the neural basis of perceptual decisions about the position-in-depth of stimuli (Chowdhury and DeAngelis, 2008; Cowey and Porter, 1979; DeAngelis et al., 1998; Uka et al., 2005; Uka and DeAngelis, 2004). Determining the position in depth of an object is an important aspect of spatial vision, e.g., for computing the scene layout or when reaching for an object, but representing an object's 3D structure requires more than the computation of position in depth, as it entails an analysis of at least relative depth or gradients within a depth cue, such as gradients of disparity. In fact, the representation of an object's 3D structure should show some invariance with regard to its position in depth in order to function efficiently for object recognition.

Previous studies have demonstrated that IT neurons in the anterior lower bank of the superior temporal sulcus (STS) encode the 3D structure of disparity-defined 3D surfaces (Janssen et al., 1999, 2000). Notably, these neurons demonstrated selectivity for relatively simple 3D structures such as convex and concave surfaces and this structure selectivity was present at different positions in depth of the surface. The importance of 3D-structure information for object encoding in IT was demonstrated by a recent study showing that a large proportion of IT neurons lost their selectivity when 3D-structure information, including disparity, was removed from the stimulus (Yamane et al., 2008).

Recently, by recording in the anterior STS region of IT while monkeys performed a disparity-defined 3D-structure-categorization task, we have demonstrated that the activity of 3D-structure-selective neurons correlates with the subject's choice during the time period wherein perceptual decisions about 3D structures are formed (Verhoef et al., 2010). This observation, together with the invariance for size and position (in depth)

observed in 3D-structure-selective neurons (Janssen et al., 2000), is compatible with these 3D-structure-selective IT neurons playing a central role in disparity-defined 3D-structure categorization, yet causal evidence for such a role has been lacking.

Previous studies employed microstimulation to examine a causal link between the neural activity within an area and a behavior of interest. In the visual domain, most microstimulation studies examining the role of neurons with particular stimulus selectivities have focused on areas in the dorsal visual stream. For instance, these studies have shown that neurons in MT contribute to the discrimination of motion direction and absolute disparity (Salzman et al., 1990; DeAngelis et al., 1998), and neurons in MST contribute to motion-direction discrimination (Celebrini and Newsome, 1995) and the perception of heading from optic flow (Britten and van Wezel, 1998), as do neurons in area VIP (Zhang and Britten, 2011). In contrast, the ventral visual stream has been largely neglected despite its presumed role in object recognition and categorization. One notable exception is a study by Afraz et al. (2006), who found that microstimulation of clusters of face-selective IT neurons influenced behavior in a task in which monkeys categorized between images of faces and nonface images. This study provided causal evidence for the conjecture that IT neurons encoding particular object information subserve perceptual categorization in tasks designed to rely on such object information. The findings of this study raise several important questions. First, is the activity of IT neurons causally linked to shape categorization in general, e.g., also for simple shape discrimination, or do faces form a special case? Second, does IT only subserve high level categorization (e.g., faces versus nonfaces), or does it underlie finer categorizations as well? For example, is IT also important for categorization within a class of objects such as faces of different individuals or specific 3D objects? Third, given the complexity of the face and nonface stimuli in Afraz et al. (2006), it is unclear which visual feature(s) was used by the monkeys to solve the task and drove the neurons. Disparity-defined stimuli present a nice opportunity to link perceptual and neural features since both the monkeys and the neural activity are unable to discriminate between different disparity-defined stimuli without extracting the 3D information encoded in the gradients of binocular disparities, i.e., no other cues are available. Finally and related to the previous point, it is still unclear whether IT codes information about the 3D-structure of objects for categorization purposes. In the present study, we seek answers to these questions.

We electrically microstimulated clusters of IT neurons having a particular 3D-structure preference (i.e., convex or concave) while monkeys were categorizing 3D structures as convex or concave. We were able to strongly and predictably influence both the monkey's choices and the time taken to reach those decisions. These findings demonstrate that IT neurons are causally implicated in the categorization of 3D structures.

## RESULTS

We trained two rhesus monkeys (M1 and M2) to report the 3D structure of a static random-dot stereogram. The stereograms depicted either a concave or convex surface which was presented at one of three positions in depth, i.e., in front of, behind, or within the fixation plane. This procedure enforces the use of perceptual strategies that are based on disparity variations within the stimulus (i.e., disparity gradients or curvature) rather than strategies relying on position-in-depth information (i.e., "near" or "far" decisions; see Verhoef et al. [2010]). We controlled the difficulty of the task by manipulating the percentage of dots defining the 3D surface, henceforth denoted as the percent stereo-coherence. The monkey was free to indicate its choice at any time after stimulus onset by means of a saccade to one of two choice-targets (Figure 1). In addition to choice-behavior, this procedure allowed us to measure reaction times (RTs; see Experimental Procedures), and it demarcates the perceptual decision process more precisely in time. The average RT on nonstimulated trials was 242 ms and 353 ms for monkey M1 and M2, respectively.

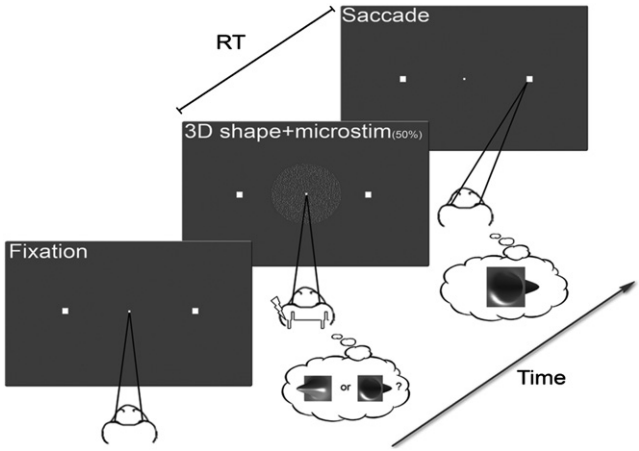


**Figure 1. Task**

Following fixation, a static random-dot stereogram portraying either a concave or convex surface was presented on a screen. The monkey indicated whether he perceived a convex or concave 3D structure by means of a saccade to one of two choice-targets positioned to the left and right of the fixation dot. The monkey was free to indicate its choice at any moment after stimulus onset. Microstimulation was applied on half of randomly chosen trials, starting 50 ms after stimulus onset and ending whenever the monkey left the fixation window. See also Figure S1.

We asked whether electrical microstimulation in clusters of 3D-structure-selective IT neurons could influence the monkey's behavioral choices and RTs during a 3D-structure categorization task in a manner that is predictable from the 3D-structure preference of neurons at the stimulated site. Microstimulation is a powerful tool for establishing causal relationships between physiologically characterized neurons and behavioral performance (Afraz et al., 2006; Britten and van Wezel, 1998; DeAngelis et al., 1998; Hanks et al., 2006; Romo et al., 1998; Salzman et al., 1990). However, the electrical pulses evoked by microstimulation simultaneously excite many neurons in the neighborhood of the electrode tip (Histed et al., 2009; Tehovnik et al., 2006). Therefore, successful application of microstimulation relies upon structural regularities within the cortex, such as

a clustering of neurons with comparable stimulus selectivities (Afraz et al., 2006; DeAngelis et al., 1998).

### Clustering of 3D-Structure-Selective Neurons in IT

Since it was unknown whether neurons with similar 3D-structure preferences cluster in IT, we started each experimental session by assessing the 3D-structure preference of multiunit activity (MUA) at regularly spaced intervals (steps of ~100–150 μm) along the cortex. We measured 3D-structure selectivity in a total of 772 MUA sites (see Figure S2 available online for the distribution of their selectivities). Note that the electrode penetrated the cortex in the lower bank of the anterior STS approximately orthogonal to the surface. At each cortical position, we determined the 3D-structure selectivity of the MUA using a passive fixation task in which the monkey viewed 100% stereo-coherent convex or concave stimuli positioned at one of three positions in depth. On different trials, stimuli were positioned either behind (Far), within (Fix), or in front of (Near) the fixation plane. We observed that neurons with similar structure preferences, i.e., convex or concave, clustered together with an observed maximum vertical extent of 1 mm and an average vertical extent of 360 μm (SEM, 37 μm) and 540 μm (SEM, 59 μm) for monkey M1 and M2, respectively (see Figure 2A for an example and Figure S3 for a summary of all clusters). These estimates are most likely biased due to cortical instabilities (i.e., gradual rise of the cortex after electrode penetration), attachment of the cortex to the electrode and time constraints (i.e., we could not always sample the entire vertical extent of the lower bank STS within a single penetration). Nonetheless, these data show that neurons with similar 3D-structure preferences are spatially organized in IT, as they are for 2D-shape features (Fujita et al., 1992).

Once we encountered a 3D-structure-selective neuronal cluster, we positioned the electrode in the estimated center of that cluster and once more verified the 3D-structure selectivity ($p < 0.05$; main effect of structure in an ANOVA with structure and position in depth as factors) before starting the 3D-structure-categorization task (see also Experimental Procedures). The MUA at the center-position of these clusters displayed marked 3D-structure selectivity. To illustrate this, Figures 2B and 2C show the average spike-density function of all 3D-structure-selective sites (n = 34; monkey M1: n = 16; monkey M2: n = 18) for the preferred and nonpreferred structure, for each position in depth and each monkey separately. For each 3D-structure-selective site, the preferred structure was defined as the structure with the highest average MUA in the stimulus interval [100 ms, 800 ms] (0 = stimulus onset; see Experimental Procedures for further details). Hence, Figures 2B and 2C show that, in agreement with previous single-cell studies (Janssen et al., 1999, 2000; Yamane et al., 2008), 3D-structure preference generalized well over position in depth across our population of 3D-structure-selective MUA sites. We observed significantly more convex-preferring neuronal clusters (n = 27) compared to concave-preferring clusters (n = 7; $p < 0.001$, binomial test). This convexity bias is a known property of IT neurons (Yamane et al., 2008) and agrees with natural image statistics (e.g., objects tend to be globally convex) and with the superior psychophysical performance observed for convex stimuli (Philips and Todd, 1996).

### Microstimulation of Clusters of 3D-Structure-Selective IT Neurons

We observed clustering of IT neurons with a similar 3D-structure preference in 33 electrode penetrations. Except for one penetration, we only microstimulated at a single position within a cluster. For the cluster in which we stimulated twice (convex selective; cluster size = 900 μm), stimulation positions were separated by ~450 μm. Since stimulation positions were well separated within this cluster, the findings of these two positions are reported individually. During the 3D-structure discrimination trials, we applied microstimulation (35 μA, 200 Hz; see Experimental Procedures) on half of these trials, chosen randomly. Stimulation started 50 ms after stimulus onset and ceased when the monkey's gaze left the fixation window to indicate his choice. The average microstimulation duration was 194 ms and 306 ms in monkey M1 and M2, respectively. Microstimulation strongly biased the monkey's choice toward the preferred 3D structure of the stimulation site. Figures 3A and 3B show the effect of microstimulation for two example sites. These plots portray the proportion of choices (~35 trials per data point) favoring the preferred structure of the 3D-structure-selective site (i.e., preferred choices) as a function of stereo-coherence for trials with (red) and without (blue) microstimulation. By convention, positive stereo-coherences are used for the preferred structure (Figure 3A, convex; Figure 3B, concave) while negative stereo-coherences relate to the nonpreferred structure of a 3D-structure-selective site. In the absence of microstimulation, preferred structures at higher stereo-coherences were associated with a higher number of preferred choices, while coherent nonpreferred structures elicited more nonpreferred choices, as expected from the stereo-coherence manipulation. Importantly, these plots show that microstimulation markedly increased the proportion of preferred choices. We used logistic regression analysis (average $R^2$ across sites = 0.93; see Experimental Procedures) to quantify the effect of microstimulation. The fitted logistic functions are shown in Figures 3A and 3B for the two example sites and reveal a clear leftward shift, i.e., toward more preferred choices, of the psychometric function on trials with (red solid line) compared to those without (blue solid line) microstimulation.

It is convenient to quantify the microstimulation-induced horizontal shift of the psychometric function by the proportion of coherent dots (% stereo-coherence) that must be added to the random-dot stereograms to produce a comparable shift in behavior (see Experimental Procedures). Figure 3C shows a histogram of the psychometric shifts, expressed as percent stereo-coherence, observed over all 3D-structure-selective sites. We observed a significant shift (Wald test; $p < 0.05$) toward more preferred choices in 24 out of 34 (~71%) 3D-structure-selective sites (black bars in Figure 3C; M1: 14 out of 16; M2: n = 10 out of 18). The average shift of 22% stereo-coherence in the direction of more preferred choices was significantly different from zero ($p < 0.0001$, bootstrap test). For comparison, a 22% change in the stereo-coherence of the disparity stimulus without microstimulation corresponded to a shift in behavioral performance from random (50% correct) to almost 80% correct. The shift was significant for each monkey ($p < 0.0001$; insets in Figure 3C). Microstimulation induced significant psychometric shifts toward more preferred choices in 17 out of 27

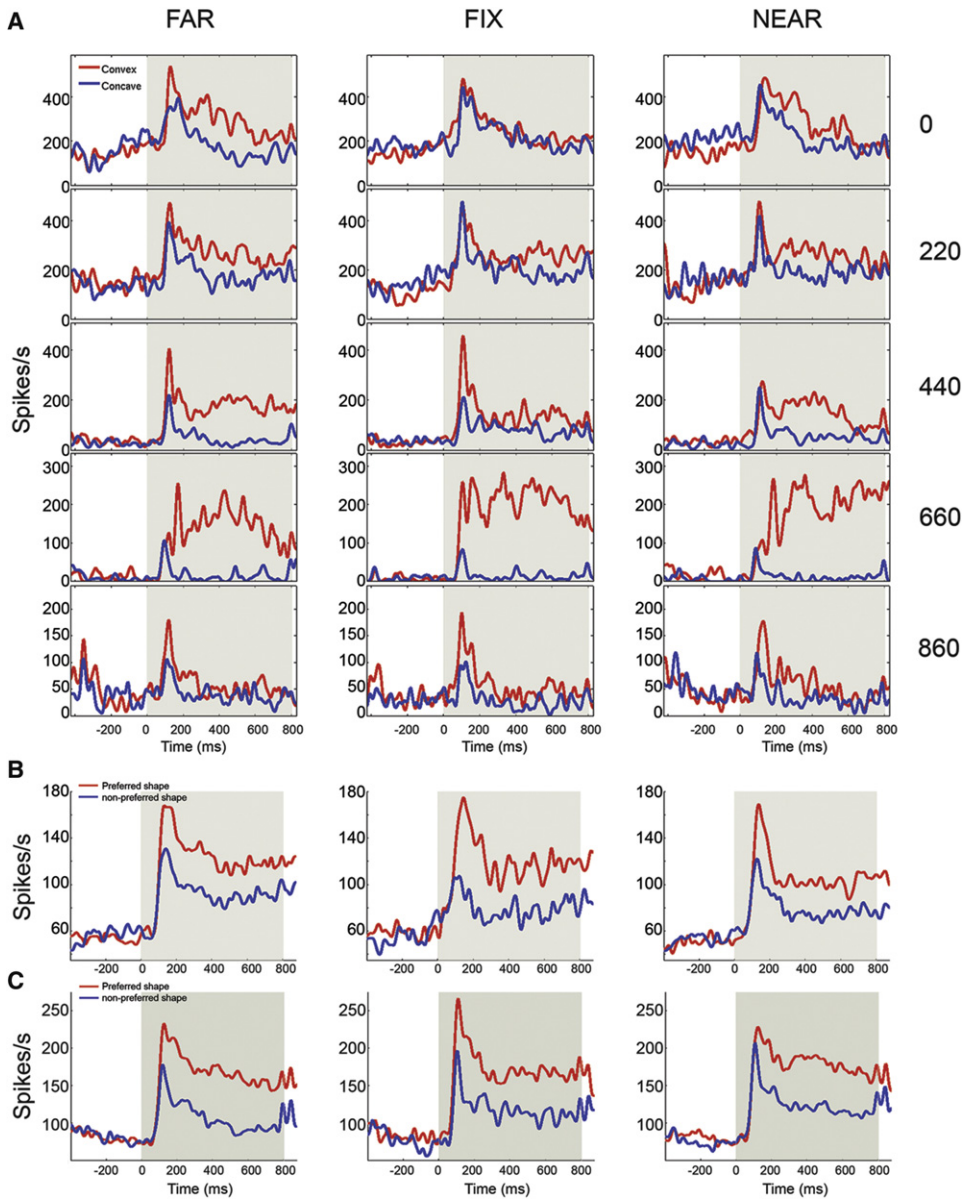


**Figure 2. 3D-Structure Selectivity and Clustering in IT**

(A) Each row shows the average spike-density function based on the MUA for the preferred (convex; red) and the nonpreferred (concave; blue) structure for a particular electrode position in a convex-selective cluster of monkey M2. The number on the right of each spike-density plot indicates the depth of the electrode position relative to the start of the 3D-structure-selective cluster. We additionally observed 3D-structure-selective MUA at other positions within this cluster (i.e., 120, 320, and 760 μm), but these positions are not shown for plotting purposes. This 3D-structure-selective cluster was preceded by 600 μm of responsive MUA that was nonselective for 3D structure. Due to time limitations, we did not sample the cortex further than 860 μm into the 3D-structure-selective cluster. Hence, it is possible that the vertical size of this 3D-structure-selective cluster extended beyond the observed 860 μm.

(B and C) Average spike-density plots based on the MUA related to the preferred (red) and nonpreferred (blue) structure of all 3D-structure selective sites (B, monkey M1; C, monkey M2). Far, Fix, and Near labels represent stimuli presented behind, within, or in front of the fixation plane, respectively. The shaded area indicates the stimulus period.

See also Figure S2 and S3.

convex-selective sites (average shift = 17%) and in all concave-selective sites (average shift = 41%). The association between the 3D-structure preference of a site and the direction of the psychometric shift due to microstimulation was highly significant when the analysis was restricted to all sites for which we observed a significant stimulation-induced shift of the psychometric function ($n = 24$, $p < 0.0001$; monkey M1: $n = 14$, $p < 0.001$; monkey M2: $n = 10$, $p = 0.01$; Fisher exact test), or when including all 3D-structure-selective sites ($n = 34$; $p < 0.0001$; monkey M1: $n = 16$, $p = 0.0001$; monkey M2: $n = 18$,

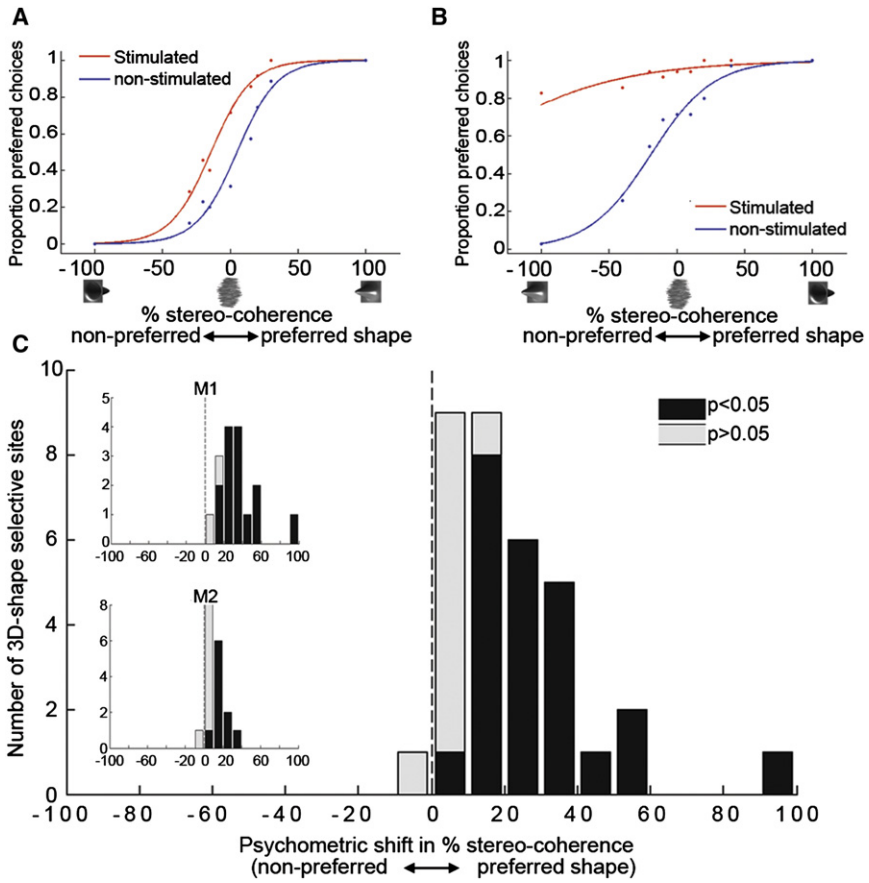


**Figure 3. Effect of Microstimulation of IT on Choice Behavior**

(A) Choice-data from a convex-selective example site in monkey M2 and (B) a concave selective example site in monkey M1. The plots show the proportion of choices that matched the preferred structure of the 3D-structure-selective site (preferred choices) as a function of stereo-coherence for trials with (red) and without (blue) microstimulation. Positive and negative stereo-coherences relate to the preferred and non-preferred structure, respectively. Solid lines show the fitted psychometric functions. Microstimulation shifted the psychometric function toward more preferred choices by (A) 19% ($p < 0.001$) and (B) ~94% ($p < 0.001$) stereo-coherence, our strongest effect. Note that in (B), microstimulation caused the monkey to respond concave on almost every trial, even when a perfectly smooth (100% stereo-coherence) convex stimulus was presented, which the monkey categorized almost perfectly in the absence of microstimulation.

(C) Histogram of microstimulation effects ($n = 34$ 3D-structure selective sites) expressed as a shift of the psychometric function in terms of percent stereo-coherence. Positive values are used for psychometric shifts toward more preferred choices. Black bars indicate sites with a significant shift of the psychometric function due to microstimulation ($p < 0.05$). Insets show the data from monkey M1 ($n = 16$) and M2 ($n = 18$) separately. See also Figure S3.

$p = 0.003$; Fisher exact test). Similarly, the distribution of the stimulation-induced psychometric shifts of the convex-selective sites differed significantly from that of the concave-selective sites ($p < 0.0001$ for both monkeys; permutation test with positive and negative values for shifts toward convex and concave choices, respectively). In only 1 of the 34 3D-structure-selective sites did microstimulation produce a shift (−4%) toward more nonpreferred choices, but even this was not significant ($p > 0.05$). Hence, stimulation at convex-selective sites increased the proportion of convex choices, while stimulation at concave-selective sites increased the proportion of concave choices.

We examined whether the effect of microstimulation varied with stereo-coherence using an additional interaction term in the logistic model (see Experimental Procedures). We observed a significant interaction in 14 ($p < 0.05$; Wald test; M1: 6 out of 16; M2: 8 out of 18) of the 34 3D-structure selective sites. In all but one of the sites with a significant interaction term, we noticed that microstimulation decreased the slope of the psychometric function. This dependency of the microstimulation effect on stereo-coherence at some sites hampers the ability to express the effect of microstimulation in terms of % of stereo-coherence. However, including the interaction term in the logistic model did not alter our conclusions. In fact, for the model with the interaction term, we observed that in 28 out of 34 (82%) 3D-structure-selective sites microstimulation induced a shift of the psychometric function toward an increased number of preferred choices (M1: 15 out of 16; M2: 13 out of 18). That is, some microstimulation effects that were marginally significant ($p \leq 0.08$) in the logistic model with no interaction term became significant due to the lower error variance for models that included the interaction term. Considering the logistic model with the interaction term and the population of all 3D-structure-selective sites, the average $\beta_1$-coefficient that measures the microstimulation induced bias on the monkey's choices (see Experimental Procedures), was positive (i.e., toward more preferred choices) and the difference from zero was highly significantly ($p < 0.00001$; permutation test). Using the logistic model with interaction term, we also tested for a significant $\beta 1$-coefficient for the convex- and concave-selective sites separately. For both data selections we found an average $\beta 1$ coefficient that was significantly larger than zero ($p < 0.001$, t test across monkeys), indicating a significant shift of the psychometric function toward more preferred choices for convex- and concave-selective sites. Finally, there was no significant difference between the $\beta 3$ coefficient (indicating the slope change due to microstimulation) of the convex- and the concave-selective sites ($p = 0.14$, t test). Hence, slope changes were similar among convex- and concave-selective sites.

Both monkeys displayed a small but significant response bias toward concave choices equivalent to on average 5.5% stereo-coherence ($p < 0.01$; logistic regression analysis on

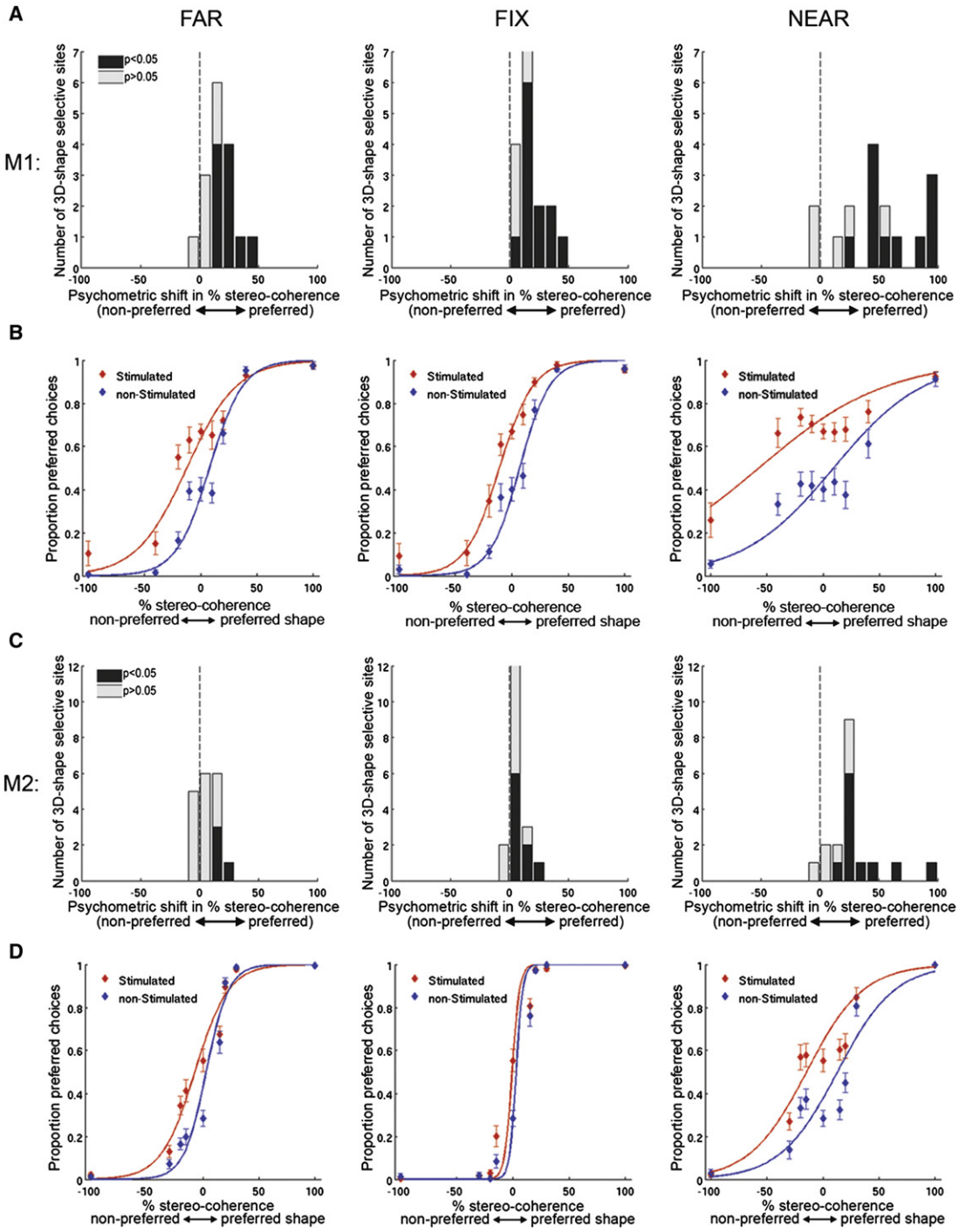


**Figure 4. Effect of Microstimulation for Each Position in Depth**

(A and C) Histograms of microstimulation effects (n = 34 3D-structure-selective sites) expressed as a shift of the psychometric function in terms of percent stereo-coherence. From left to right the data are shown for stimuli presented behind (Far), at (Fix), or in front of (Near) the fixation plane respectively. (A) and (C) show the histograms for monkey M1 (n = 16) and M2 (n = 18), respectively. For each position in depth, black bars indicate sites with a significant stimulation-induced psychometric shift ($p < 0.05$). The preferred structure was determined in the same manner as for Figure 3c.

(B and D) show the average psychometric function across all 3D-structure-selective sites for each position in depth and for stimulated (red) and nonstimulated (blue) trials for monkey M1 and M2, respectively. Vertical bars indicate ± 1 SEM. Stimulation effects were generally stronger for low-coherent, i.e., more difficult stimuli. Most likely this explains why microstimulation effects were also stronger for Near stimuli, since each monkey's behavioral performance was poorer for such stimuli. For the 0% stereo-coherent stimuli, the dot-disparity was randomly chosen from a range that covered the entire extent of the disparities of the non-zero stereo-coherent stimuli (see Experimental Procedures). We therefore combined the data from each position in depth with those of the 0% stereo-coherent stimuli.

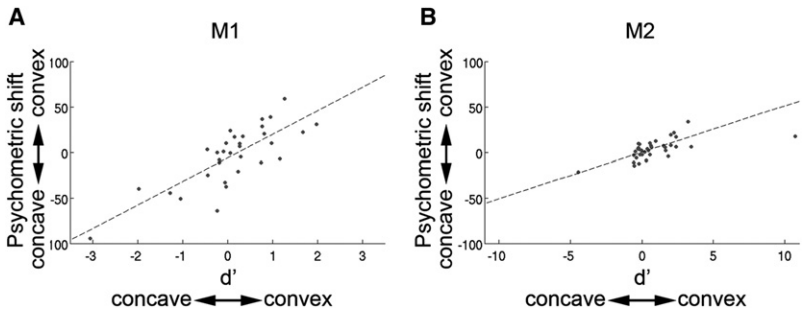


**Figure 5. Shift of the Psychometric Function Plotted against the 3D-Structure Selectivity of the MUA Measured at Each Stimulation Site**

Positive and negative psychometric shifts denote shifts toward more convex and concave choices, respectively. Signed d′ values are used to point out the 3D-structure preference of the MUA-sites, with positive and negative values indicating convex and concave preferences, respectively (see Experimental Procedures). (A) monkey M1 (n = 32). (B) Monkey M2 (n = 36). The black dashed lines are robust regression lines (M1: slope = 25.9, $p < 0.001$; M2: slope = 5.1, $p < 0.001$; none of the intercepts differed significantly from zero, $p > 0.05$). See also Figure S4.

3D-structure-selective and -nonselective sites with no significant effect of microstimulation to avoid misestimating the response bias due to e.g., probability matching effects [Salzman et al., 1992]. If microstimulation in IT elicited activity that was unrelated to the sign of the 3D structure (that is, concave versus convex 3D structure), the task would be expected to become more difficult and the monkey would most likely rely more heavily on his response bias to make a choice, i.e., to choose concave. One would therefore expect a higher proportion of stimulation-induced psychometric shifts toward more concave choices. Nevertheless, we observed stimulation-induced psychometric shifts toward convex choices in 96% of all convex-selective sites. Hence, considering the convex 3D-structure-selective sites, our results cannot be explained by an activation of the monkeys' response bias, since this would have produced shifts in the opposite, concave direction.

Microstimulation significantly biased the monkey's choice toward more preferred choices at each of the three positions-in-depth of the stimulus ($p < 0.0001$ for Far-, Fix-, and Near-position-in-depth; Figures 4A and 4B, M1; Figures 4C and 4D, M2). In addition, the strength of the microstimulation effect tended to increase with the 3D-structure selectivity of a site. Figure 5 shows the shift of the psychometric function plotted against the 3D-structure selectivity of the MUA measured at each stimulation site. For this purpose, negative and positive psychometric shifts denote shifts toward more concave and convex choices, respectively. Signed d′-values measure the 3D-structure preference of the MUA-sites, with positive and negative values indicating convex and concave preferences, respectively (see Experimental Procedures). We observed a significant correlation between the signed d′ and the signed psychometric shift in each monkey (M1: 0.79, $p < 0.001$; M2: 0.62, $p < 0.001$). The previous analysis is based on all 68 sites in which we stimulated, including 34 sites not selective for 3D shape (see below). However, when restricting the analyses to the 34 3D-structure-selective sites, a similar trend was present as we observed a correlation between the magnitude of 3D-structure selectivity ($|d'|$) and the unsigned stimulation-induced psychometric shift of 0.74 and 0.35 for monkey M1 and M2, respectively (M1: $p = 0.001$; M2: $p = 0.15$; Fisher Z test; see Figure S4).

Across all 34 3D-structure-selective sites, 22 sites (65%) contained at least one electrode position for which the MUA was significantly 3D-structure-selective at each position in depth ($p < 0.05$, t test). Ten (75%) of the remaining 12 sites contained at least one electrode position for which the MUA was significantly 3D-structure-selective for two positions in depth ($p < 0.05$, t test). In none of the 3D-structure-selective sites did we observe a significant reversal in structure preference at any position-in-depth ($p > 0.05$, t test). Hence, all 3D-structure-selective sites were characterized by only one 3D-structure preference. We tested whether stimulation in clusters containing MUA positions with significant selectivity for all positions-in-depth (putative completely invariant sites) caused larger microstimulation effects compared to stimulation in clusters with MUA positions that did not display significant structure selectivity at each position in depth (putative incompletely invariant sites). Stimulation in clusters with completely invariant MUA positions caused significantly larger microstimulation effects in monkey M1 (mean psychometric shift of 45% versus 19%; $p = 0.005$) but not in monkey M2 (mean psychometric shift of 12% versus 9%; $p > 0.05$), although a trend was present. Given that we probably did not only stimulate completely invariant cells and given the consistency of the microstimulation results, even in clusters with incomplete invariance ($p < 0.003$ for each monkey; t test for a significant psychometric shift toward more preferred choices), it seems possible that 3D-structure categorization does not solely rely on IT cells with complete tolerance for position-in-depth. Yet we cannot exclude the possibility that stimulation in 3D-structure selective clusters with incomplete invariance may have also stimulated nearby completely invariant structure-selective cells, from which we did not record, that caused the increase in preferred choices.

Considering only the trials in which monkeys made a preferred choice, we observed significantly shorter average reaction times on stimulated compared to nonstimulated trials (Figures 6A and 6C; M1: average RT-difference: 3 ms; $p = 0.04$; M2: average RT-difference: 11 ms; $p = 0.006$; ANOVA). Furthermore, for non-preferred-choice trials, we noticed significantly longer average reaction times on stimulated compared to nonstimulated trials (Figures 6B and 6D; M1: average RT-difference: ~5 ms; $p = 0.002$; M2: average RT-difference: ~17 ms; $p = 0.003$; ANOVA). These findings can be understood as follows: if microstimulation increases the structure evidence in favor of the preferred structure of the neurons near the stimulating electrode, microstimulation should reduce response time on preferred-choice trials. When the monkey chooses the nonpreferred structure, however, microstimulation slows down the behavioral response since the neural activity that has led to this nonpreferred choice has had to compete with stimulation-induced activity signaling that the monkey should opt for the

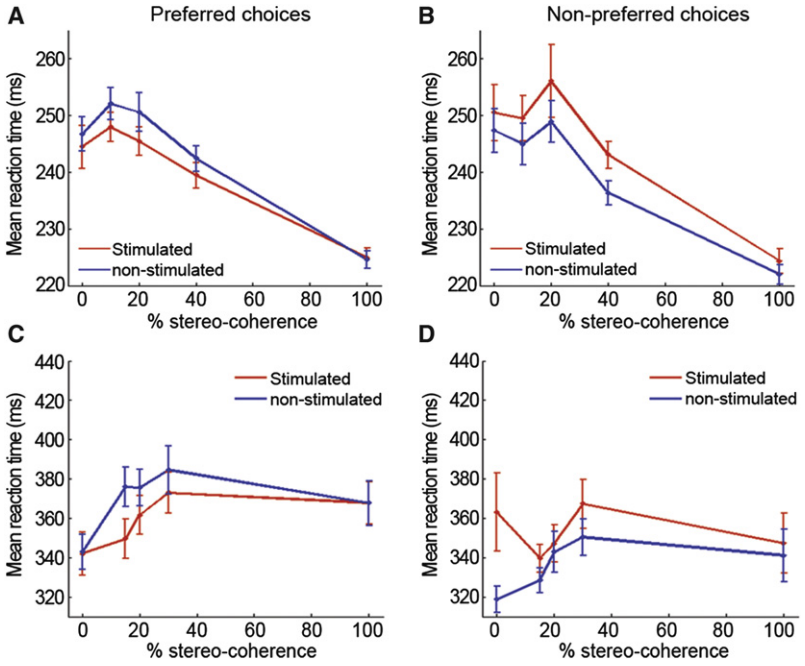


**Figure 6. Effect of Microstimulation of IT on Reaction Times**

Average reaction times as a function of stereo-coherence for stimulated (red) and nonstimulated (blue) trials.
(A) Preferred choices of monkey M1 (n = 16 sites).
(B) Nonpreferred choices of monkey M1 (n = 16 sites).
(C) Preferred choices of monkey M2 (n = 18 sites).
(D) Nonpreferred choices of monkey M2 (n = 18 sites).
Vertical lines indicate ± 1 SEM.

alternative choice. Therefore, these findings demonstrate that microstimulation was not disregarded in trials in which the monkey did not choose the preferred structure of the stimulated neuronal cluster.

The effects of microstimulation on the average reaction times were very similar for convex- and concave-selective sites. Across the 27 convex-selective sites microstimulation caused significantly shorter reaction times for preferred choices ($p = 0.008$, ANOVA across monkeys) and significantly longer reaction times for nonpreferred choices ($p = 0.002$, ANOVA). Despite the relatively small number of concave-selective sites, we observed that microstimulation significantly accelerated preferred choices ($p = 0.03$, ANOVA across monkeys) and caused a marginally significant slowing-down of nonpreferred choices ($p = 0.06$, ANOVA across monkeys). Furthermore, the interaction between the selectivity of a site (i.e., convex or concave) and the effect of microstimulation on reaction times was not significant for both preferred ($p = 0.86$, ANOVA) and nonpreferred choices ($p = 0.88$, ANOVA). The effects of microstimulation on the average reaction times were also similar for each position in depth of the stimulus. That is, we did not find a significant interaction between the effect of microstimulation on the average reaction times of each monkey and the position-in-depth of the stimulus ($p > 0.05$, ANOVA).

## Microstimulation of Clusters of 3D-Structure-Nonselective IT Neurons

Analyses of the effect of microstimulation in sites that were nonselective with regard to 3D structure provided further evidence for a relationship between the 3D-structure preference and the effect of microstimulation at a site. Indeed, if our microstimulation effects were caused by factors unrelated to the 3D-structure preference of the stimulated neurons, one would expect similar microstimulation effects at IT sites *not* selective for 3D structure. Therefore, we also stimulated in 34 sites that were not selective for 3D structure (M1: n = 16; M2: n = 18), recorded at the same grid positions as the 3D-structure-selective sites. We observed some variability in the functional properties of the MUA recorded on different days in the same grid position, most likely because of the long and therefore somewhat variable trajectory traversed by the electrode before reaching the IT cortex. The 3D-structure-nonselective sites often contained 3D-structure-selective single neurons, but without clustering. For microstimulation purposes, however, we stimulated only sites that were neighbored by MUA positions with no 3D-structure selectivity for at least 125 μm in either direction (i.e., up- and downwards). Thirty-two of the thirty-four 3D-structure-nonselective sites contained neurons responsive to our stimuli ($p < 0.05$, ANOVA). For the nonselective sites, preferred and nonpreferred choices were undefined. In an initial analysis, we defined positive and negative stereo-coherences for convex and concave structures, respectively. For the nonselective sites, we observed an average shift of −5% (i.e., in the direction of concave choices; Figure 7) that did not differ significantly from zero ($p = 0.98$; M1: $p = 0.9$; M2: $p = 0.72$; bootstrap test). We also repeated analyses identical to those of the 3D-structure-selective sites. That is, we determined the sign of the stimulation-induced psychometric shifts based on the putative (because nonsignificant) 3D-structure selectivity of a site, i.e., the 3D structure giving the strongest response (see above; positive [negative] shifts are shifts in the putative (non)preferred direction). The average psychometric shift of 3.7% (3.2% for responsive but 3D-structure-nonselective sites) computed by this method did not differ significantly from zero ($p > 0.05$). Similarly, there was no significant association between the putative 3D-structure preference of a site and the direction of the psychometric shift due to microstimulation ($p > 0.05$; Fisher exact test), and the distribution of the stimulation-induced psychometric shifts of the putative convex-selective sites did not differ significantly from that of the putative concave-selective sites ($p > 0.05$; permutation test with positive and negative shifts for shifts toward convex and concave choices, respectively). The distribution of microstimulation effects of the non-3D-structure selective sites differed significantly from those of either the convex- or concave-selective sites, the distribution being more biased toward more convex or concave choices for the convex and concave selective sites,

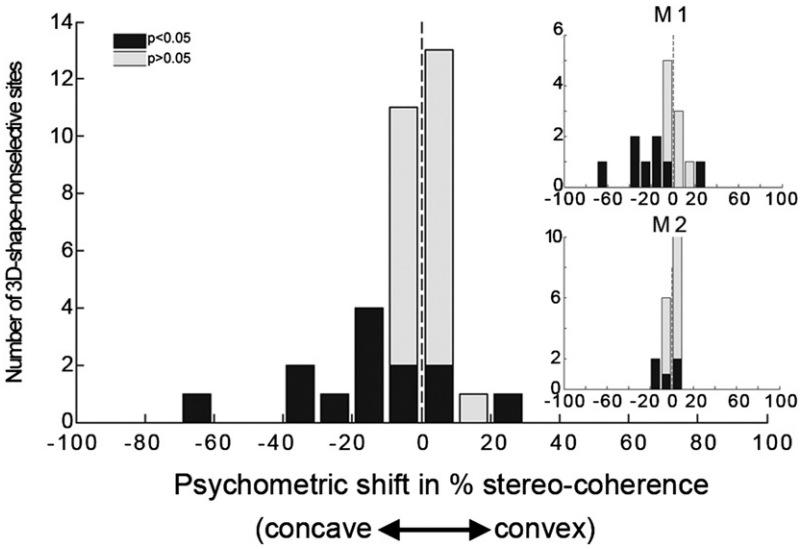


**Figure 7. Effect of Microstimulation in 34 Sites Not Selective for 3D Structure**

Positive and negative stereo-coherences are used for convex and concave structures, respectively. Black bars indicate sites displaying a significant shift of the psychometric function due to microstimulation ($p < 0.05$). Insets show the data from monkey M1 (n = 16) and M2 (n = 18) separately.

respectively ($p < 0.01$ for both monkeys; permutation test). Note, however, that we did observe significant effects of microstimulation for some nonselective sites (black bars in Figure 7; M1: n = 8; M2: n = 5). Two such significant effects were observed in the two unresponsive non-3D-structure selective sites (−9% in monkey M1 and −15% in monkey M2; toward concave choices; $p < 0.05$). Such significant effects can be explained as follows: first, we could examine only the 3D-structure selectivity of recording positions in the vertical direction, and had limited knowledge of 3D-structure selectivity along the horizontal direction. Furthermore, electrical current diffuses spherically, i.e., in all directions and with effects (i.e., activated neurons) at distances of up to several millimeters (Butovas and Schwarz, 2003; Histed et al., 2009). As a result, the behavioral effects of microstimulation at nonselective sites may have been the result of activation of neighboring or distant 3D-structure-selective neurons. In monkey M1, we also stimulated in four responsive but non-3D-structure-selective sites located ~3–4 mm anterior to the 3D-structure-selective recording positions and observed a significant effect of microstimulation in one of these sites (shift = −11%; toward concave; $p = 0.02$). In this case, it is still possible that we stimulated some concave-preferring neurons. However, a second factor related to the response bias of the animals might also explain this stimulation effect: both monkeys displayed a moderate response bias toward concave (see above) which was mainly present at lower stereo-coherences, i.e., under noisy perceptual conditions. If microstimulation of non-3D-structure-selective sites added noise to the perceptual process, this could result in an increased tendency to respond "concave." Correspondingly, microstimulation in non-3D-structure-selective sites shifted the psychometric function predominantly, but nonsignificantly ($p > 0.05$, binomial test), in the concave direction (see Figure 7).

We also examined the effect of microstimulation at 3D-structure-nonselective sites upon the average RTs during the task. For this purpose, we sorted the trials according to the direction of the stimulation-induced psychometric shift. For instance, when microstimulation induced a shift toward increased convex choices, trials in which the monkey chose "convex" and "concave" were considered "preferred" and "nonpreferred" choices, respectively. For both preferred and nonpreferred choices, we observed no significant difference between the average RTs of stimulated and nonstimulated trials ($p > 0.05$ for each monkey, ANOVA on all nonselective sites; $p > 0.05$ across monkeys, ANOVA on all nonselective sites with a significant stimulation-induced psychometric shift; n = 13). Interestingly, this result shows that, even when microstimulation in nonselective sites occasionally increased the probability of a certain choice, it did not facilitate these choices nor delay the opposite choices. Indeed, any such effects upon the average RTs occurred only in the 3D-structure-selective sites, thereby confirming the specificity of the microstimulation effects at the 3D-structure-selective sites.

## DISCUSSION

When objects are viewed, the brain computes their 3D structures from the retinal activity maps of the two eyes. To our knowledge, our findings provide the first causal evidence relating a specific brain area to 3D-structure perception. We show that microstimulation of clusters of 3D-structure-selective IT neurons increased the proportion of choices corresponding to the preferred 3D structure of the stimulated neurons and additionally facilitated such choices while impeding nonpreferred choices. Note that the magnitude and the consistency of the microstimulation effects are striking, considering that we applied unilateral stimulation in an area with bilateral receptive fields.

Understanding the specific roles of the numerous cortical areas processing disparity is a considerable and open challenge (Anzai and DeAngelis, 2010; Chandrasekaran et al., 2007; Nienborg and Cumming, 2006; Parker, 2007; Preston et al., 2008; Umeda et al., 2007). Earlier studies have focused on tasks in which monkeys were instructed to discriminate the depth (near versus far) (Cowey and Porter, 1979; DeAngelis et al., 1998; Nienborg and Cumming, 2009; Uka et al., 2005) or orientation of a disparity-defined surface (Tsutsui et al., 2001). These studies have shown that neurons in the middle temporal area MT (DeAngelis et al., 1998) and the IT (Cowey and Porter, 1979) cortex contribute to the coarse discrimination of the position-in-depth of stimuli, while the caudal intraparietal area CIP may be causally involved in 3D-orientation discrimination (Tsutsui et al., 2001). Our findings advance our understanding of disparity processing

by demonstrating a causal involvement of IT in disparity-defined 3D-structure categorization.

Our task required monkeys to categorize between convex and concave 3D structures which could be disrupted by spatially uniform disparity noise. As noise increased, solving the task most likely necessitated the pooling of relative disparities across the stimulus in order to extract the signal from the noise. Such perceptual processes in which an image is constructed based on the relative disparities at different positions may engage processes similar to those underlying 3D-shape perception in which spatial gradients of disparity are used to infer the 3D shape of an object. Hence, monkeys could have solved the task by extracting the 3D shape of the stimulus. Furthermore, previous studies have shown that neurons in IT encode the depth profile of a stimulus, not merely relative depth (Janssen et al., 2000; Yamane et al., 2008). These arguments suggest that microstimulation of 3D-structure-selective IT neurons might have influenced 3D-shape-categorization behavior. Alternatively, monkeys could have relied on lower-order information on the relative depth within the stimulus. Specifically, it is possible that monkeys ignored the smooth disparity gradients within the stimulus while retaining the relative position of the center of the stimulus with respect to the surround. In this respect, a previous study found that microstimulation of disparity-selective MT cells biased absolute-disparity discrimination but had no influence on relative-depth discrimination (Uka and DeAngelis, 2006). Our findings show that IT neurons, at the very least, subserve relative-depth discrimination which could point to a basic dissociation between the dorsal and the ventral visual pathway.

We have previously shown that the correlation between neuronal activity in IT and behavioral choice during 3D-structure categorization arises shortly after stimulus onset and decreases before stimulus offset (Verhoef et al., 2010). These dynamics and the moderate magnitude of this correlation (similar to those in other sensorial areas such as MT) suggest that IT neurons provide perceptual evidence for decisions about disparity-defined 3D structures, rather than representing the decision variable itself (Hanks et al., 2006). Here, we have shown that microstimulation increased the RTs for nonpreferred choices, which indicates that 3D-structure-selective neurons even participate in perceptual decisions resulting in nonpreferred choices. Accordingly, our findings agree with models that explain the formation of perceptual decisions based on weighted evidence originating from opponent neural populations, in our case one with convex- and another with concave-selective neurons, that directly or indirectly influence each other's input into the decision stage, via e.g., lateral or feed-forward inhibition (Ditterich et al., 2003).

We observed clusters of IT neurons preferring either convex or concave 3D structures. Most likely, not all neurons within these 3D-structure-selective clusters represented exactly the kind of 3D structures that we employed in this study (i.e., Gaussian radial basis surfaces). Indeed, a previous study has shown that IT neurons can also encode more complex 3D structures than the ones used in our study (Yamane et al., 2008). Therefore, it seems likely that the neurons within each 3D-structure-selective cluster encode for different (complex) 3D structures but at the same time share some preference for convex or concave 3D structures. This suggests that IT neurons with specific 3D-structure preferences could not only join forces to subserve categorization of a global (nonaccidental) 3D-structure characteristic (i.e., convex or concave) but potentially also underlie more specific 3D-structure identification. Such a proposal implies a flexible readout of IT neuronal activity according to the demands implied by the task at hand.

In agreement with this proposal, previous studies have suggested that the activity of IT neurons can be read out to perform visual object categorization at various levels. For example, IT neurons could underlie categorization at the basic or ordinate level (e.g., faces versus cars) but could also provide information in support of finer categorizations, that is, subordinate classifications (e.g., differentiating between different faces, cars or dogs) (Hung et al., 2005; Kiani et al., 2007; Logothetis and Sheinberg, 1996; Riesenhuber and Poggio, 1999; Thomas et al., 2001). A previous study showed that microstimulation in clusters of face-selective IT neurons can affect a monkey's behavioral choice when categorizing images of faces versus nonface images (Afraz et al., 2006). Our findings demonstrate that neurons in IT can also subserve finer classifications, since microstimulation in IT strongly affected visual categorization at the subordinate level, i.e., for object surfaces that differed only in the sign of their curvature. Moreover, in view of the strong stimulation effects and its high position within the cortical hierarchy, this IT region might be one of the final regions where disparity-defined 3D-structure characteristics such as the sign of the curvature are processed before being read out by decision-related areas.

## EXPERIMENTAL PROCEDURES

### Subjects and Surgery

Two male monkeys (*Macaca mulatta*) served as subjects. Monkey M1 participated in an earlier study in which we observed decision-related neural activity in IT while performing the 3D-structure discrimination task (Verhoef et al., 2010). Recording cylinders were implanted under isoflurane anesthesia and aseptic conditions. Each monkey received a recording cylinder (Crist Instrument) that was positioned above the right anterior IT cortex. All surgical procedures and animal care were approved by the K.U. Leuven Ethical Committee and in accordance with the European Communities Council Directive 86/609/EEC. Structural MRI (0.6 mm slice thickness) using glass capillaries filled with a 1% copper sulfate solution and inserted into several grid positions and the pattern of gray-to-white matter transitions, confirmed that the recordings were made in the anterior part of the lower bank of the STS (Horsley-Clark coordinates (across monkeys): 15–17.5 mm anterior, 22–25 mm lateral).

### Stimuli and Task

The stimulus set consisted of static random-dot stereograms with 8 different circumference-shapes (e.g., circle, ellipse, square, etc.; see Figure S1; size: ~5 degrees). Stimuli were centered foveally on a gray background. The depth structure was defined solely by horizontal disparity as a two-dimensional radial basis Gaussian surface (standard deviation = 48 pixels, 0.96 degrees) which could be either convex or concave (maximal disparity amplitude: 0.15 degrees). The dots consisted of Gaussian luminance profiles (width: 7 pixels; height: 1 pixel; horizontal standard deviation: 0.7 pixels; 1 pixel ≈0.02 deg). For each dot, the mean of the Gaussian luminance profile could be positioned along a continuous axis resulting in perceptually smooth stereograms with sub-pixel resolution. Stimuli were presented at 3 positions in depth, i.e., before, behind or at the fixation plane (±0.23 degrees depth variation). Task difficulty was manipulated by varying the percentage of dots defining the surface, i.e., the signal strength (or stereo-coherence). Dots that were not designated as defining the surface were assigned a disparity that was randomly drawn from a uniform distribution (support = [−0.50 degrees, 0.50

degrees]). For each experiment, we used 20 different random dot patterns per signal strength. Monkeys were required to maintain fixation (fixation window < 1.5 degrees on a side) on a small fixation point throughout the trial. Each trial started with a prestimulus interval, the duration of which was randomly selected from an exponential distribution (mean = 570 ms, minimum duration = 250 ms, maximum duration = 1500 ms). After stimulus onset, the monkey was free to indicate his choice at any time. Only trials having a RT > 100 ms were rewarded and included in our dataset. At the moment the monkey left the fixation window the stimulus was extinguished. Choice-targets were visible throughout the trial until one of the targets had been fixated for 300 ms. The rare trials in which monkeys fixated the choice-target less than 300 ms or switched between choice-targets were not rewarded and were not included in the data set. Correct responses were followed by a liquid reward. The correct response for a trial depended on the contingency between the 3D structure of the presented stimulus and the direction of the saccadic response made by the monkey. The 0% signal strength trials were randomly rewarded with a probability of 0.5.

### Recording of Neural and Eye Position Signals and Microstimulation Parameters

Extracellular recordings were made using tungsten microelectrodes (impedance, ~0.7 MΩ at 1 kHz; FHC). Details of the physiological recording methods have been described previously (Verhoef et al., 2010). The positions of both eyes were sampled at 1 kHz using an EyeLinkII system. Electrical pulses for microstimulation purposes were delivered using a pulse generator (DS8000; World Precision Instruments) in series with an optical stimulus isolation unit (DLS100; World Precision Instruments). Stimulation consisted of bipolar current pulse trains of 35 μA delivered at 200 Hz. We used biphasic (cathodal pulse leading) square-wave pulses with a pulse duration of 0.2 ms and 0.1 ms between the cathodal and anodal pulse (total pulse duration = 0.5 ms). Similar parameters have been used in related studies (Afraz et al., 2006; DeAngelis et al., 1998).

### Recording Procedure for the Microstimulation Experiments

We sampled IT along vertical electrode penetrations in steps of ~100–150 μm. For each of these positions, we first selected the optimal (within our stimulus set) 2D-shape outline (e.g., circle, ellipse, square, etc.; size: ~5 degrees in size) using a passive fixation task. Using this optimal 2D-shape outline, we then tested the 3D-structure selectivity of a site by presenting 100% stereo-coherent concave and convex 3D structures at one of three different positions in depth (i.e., Near, Fix, Far). We then retracted the electrode to the center of the 3D-structure selective cluster, again verified that the MUA still exhibited the same 3D-structure selectivity, and started the 3D-structure discrimination task. We used the optimal 2D-shape outline at the cluster center for the discrimination task. We adopted the following criterion for defining a 3D-structure selective cluster: The center-position of a cluster had to be neighbored by MUA-positions having the same 3D-structure selectivity for at least 125 μm in both directions (i.e., up- and downwards). Similar criteria have been used in previous studies (Hanks et al., 2006; Salzman et al., 1990; Uka and DeAngelis, 2006). If time permitted, we verified the 3D-structure selectivity once again after the microstimulation experiment. The data from four experiments were excluded from our dataset because of changes in 3D-structure selectivity observed after the microstimulation experiment. In order to maximize the amount of trials in the microstimulation experiment and to minimize the amount of cortical damage to the positions with significant 3D-structure selectivity, we did not always sample the entire extent of a 3D-structure selective cluster. Hence, our data allow us to state that 3D-structure selective clusters exist in IT but do not allow us to characterize the 3D-structure selectivity in IT in an unbiased way.

### Data Analysis

For the spike-density functions in Figures 2B and 2C, the preferred structure for each 3D-structure-selective site was defined as the structure with the highest average MUA in the stimulus interval ([100 ms, 800 ms]; 0 = stimulus onset). Averaging was performed on 50% of the trials randomly chosen from the Fix-position-in-depth presentations (i.e., stimuli presented at the fixation plane). The remaining 50% of the trials were used to calculate the spike-density function for the Fix-position-in-depth stimuli. This procedure avoids spurious 3D-structure selectivities due to MUA variability unrelated to the stimulus. Importantly, the preferred structure thus defined was used to sort the MUA of the Far- and Near-trials into preferred- and nonpreferred categories. Virtually identical results were obtained when the preferred structure was determined using the MUA from the Far- or Near-positions-in-depth. The averaged spike trains of each 3D-structure selective site were first convolved with a Gaussian kernel ($\sigma$ = 10 ms) before being averaged across sites.

We used the d′ as a measure of the 3D-structure selectivity of a site. The signed d′ is defined as $d' = (\overline{X}_{convex} - \overline{X}_{concave}) / \sqrt{S^2_{convex} + S^2_{concave}/2}$, where $\overline{X}_{convex}$ and $\overline{X}_{concave}$ are the mean multiunit responses to convex and concave stimuli, respectively, and $S^2_{convex}$ and $S^2_{concave}$ are the variances of the neural responses to convex and concave stimuli, respectively. Positive and negative values indicate convex and concave tuning respectively. The unsigned d′ is given by the absolute value of the signed d′, |d′| and indicates the magnitude of the 3D-structure selectivity.

We estimated the RT for each trial as follows: The horizontal eye-traces of each trial were first low-pass filtered (cutoff = 40 Hz) to remove high-frequency noise (Bosman et al., 2009). The resulting time series $\vec{x}_t$ was transformed into velocities using the transformation $\vec{v}_n = (\vec{x}_{n+2} + \vec{x}_{n+1} - \vec{x}_{n-1} - \vec{x}_{n-2})/6\Delta t$ ($\Delta t$ = sampling period) which represents a moving average of velocities to suppress noise. The reaction time was defined as the time point relative to stimulus onset of the first of five consecutive velocities for which the speed exceeded 50 deg/s in the same direction. Reaction times were square-root transformed before being entered into an ANOVA.

We used logistic regression to model the behavioral data as a function of stereo-coherence and the occurrence of microstimulation on a trial (Afraz et al., 2006; DeAngelis et al., 1998; Salzman et al., 1990) using the following function (glmfit; Matlab R2009a): $P = 1/1 + \exp[-(\beta_0 + (\beta_1 \cdot I) + (\beta_2 \cdot x))]$, where $P$ denotes the probability of a preferred choice, $x$ represents the level of stereo-coherence and $I$ is a binary variable which takes the values 1 and 0 on stimulated and nonstimulated trials, respectively. The $\beta_0$ and $\beta_2$ coefficients measure the response bias and slope, respectively. The $\beta_1$ coefficient measures the effect of microstimulation on the monkey's response bias. The shift of the psychometric function due to microstimulation was formalized as $\beta_1/\beta_2$. This model, in which the effect of microstimulation was modeled solely as a horizontal shift or bias, was used throughout all analyses in the main manuscript. However, we obtained very similar results when fitting a logistic model that allowed for microstimulation-induced slope changes. For this reason, we added $(\beta_3 \cdot x \cdot I)$ to the linear exponent and fitted the model as before. The latter extended model was also used for plotting purposes (see psychometric functions in Figures 3A and 3B and Figure 4).

## SUPPLEMENTAL INFORMATION

Supplemental Information includes four figures and can be found with this article online at doi:10.1016/j.neuron.2011.10.031.

## ACKNOWLEDGMENTS

We thank Inez Puttemans, Piet Kayenbergh, Gerrit Meulemans, Stijn Verstraeten, Marjan Docx, Wouter Depuydt, Marc De Paep, and Karin Winnepenninckx for assistance. We thank Steve Raiguel for comments on a previous version of this manuscript. B.-E.V. received a postdoctoral fellowship at KU Leuven (Research Fund K.U. Leuven; PDMK/10/217). This work was supported by Fonds Wetenschappelijk Onderzoek grant G.0495.05N and G.0713.09, Geneeskundige Stichting Koningin Elisabeth, Interuniversitaire Attractiepolen, Geconcerteerde OnderzoeksActies 2005/18 and 2010/19, Excellentiefinanciering 05/014 and Programmafinanciering 10/008.

Accepted: October 18, 2011
Published: January 11, 2012

## REFERENCES

Afraz, S.R., Kiani, R., and Esteky, H. (2006). Microstimulation of inferotemporal cortex influences face categorization. Nature *442*, 692–695.

Anzai, A., and DeAngelis, G.C. (2010). Neural computations underlying depth perception. Curr. Opin. Neurobiol. *20*, 367–375.

Bosman, C.A., Womelsdorf, T., Desimone, R., and Fries, P. (2009). A microsaccadic rhythm modulates gamma-band synchronization and behavior. J. Neurosci. *29*, 9471–9480.

Britten, K.H., and van Wezel, R.J. (1998). Electrical microstimulation of cortical area MST biases heading perception in monkeys. Nat. Neurosci. *1*, 59–63.

Butovas, S., and Schwarz, C. (2003). Spatiotemporal effects of microstimulation in rat neocortex: a parametric study using multielectrode recordings. J. Neurophysiol. *90*, 3024–3039.

Celebrini, S., and Newsome, W.T. (1995). Microstimulation of extrastriate area MST influences performance on a direction discrimination task. J. Neurophysiol. *73*, 437–448.

Chandrasekaran, C., Canon, V., Dahmen, J.C., Kourtzi, Z., and Welchman, A.E. (2007). Neural correlates of disparity-defined shape discrimination in the human brain. J. Neurophysiol. *97*, 1553–1565.

Chowdhury, S.A., and DeAngelis, G.C. (2008). Fine discrimination training alters the causal contribution of macaque area MT to depth perception. Neuron *60*, 367–377.

Cowey, A., and Porter, J. (1979). Brain damage and global stereopsis. Proc. R. Soc. Lond. B Biol. Sci. *204*, 399–407.

DeAngelis, G.C., Cumming, B.G., and Newsome, W.T. (1998). Cortical area MT and the perception of stereoscopic depth. Nature *394*, 677–680.

Ditterich, J., Mazurek, M.E., and Shadlen, M.N. (2003). Microstimulation of visual cortex affects the speed of perceptual decisions. Nat. Neurosci. *6*, 891–898.

Ferraina, S., Paré, M., and Wurtz, R.H. (2000). Disparity sensitivity of frontal eye field neurons. J. Neurophysiol. *83*, 625–629.

Fujita, I., Tanaka, K., Ito, M., and Cheng, K. (1992). Columns for visual features of objects in monkey inferotemporal cortex. Nature *360*, 343–346.

Hanks, T.D., Ditterich, J., and Shadlen, M.N. (2006). Microstimulation of macaque area LIP affects decision-making in a motion discrimination task. Nat. Neurosci. *9*, 682–689.

Histed, M.H., Bonin, V., and Reid, R.C. (2009). Direct activation of sparse, distributed populations of cortical neurons by electrical microstimulation. Neuron *63*, 508–522.

Howard, I.P., and Rogers, B.J. (1995). Binocular Vision and Stereopsis (New York: Oxford University Press).

Hung, C.P., Kreiman, G., Poggio, T., and DiCarlo, J.J. (2005). Fast readout of object identity from macaque inferior temporal cortex. Science *310*, 863–866.

Ito, M., Tamura, H., Fujita, I., and Tanaka, K. (1995). Size and position invariance of neuronal responses in monkey inferotemporal cortex. J. Neurophysiol. *73*, 218–226.

Janssen, P., Vogels, R., and Orban, G.A. (1999). Macaque inferior temporal neurons are selective for disparity-defined three-dimensional shapes. Proc. Natl. Acad. Sci. USA *96*, 8217–8222.

Janssen, P., Vogels, R., and Orban, G.A. (2000). Three-dimensional shape coding in inferior temporal cortex. Neuron *27*, 385–397.

Joly, O., Vanduffel, W., and Orban, G.A. (2009). The monkey ventral premotor cortex processes 3D shape from disparity. Neuroimage *47*, 262–272.

Kiani, R., Esteky, H., Mirpour, K., and Tanaka, K. (2007). Object category structure in response patterns of neuronal population in monkey inferior temporal cortex. J. Neurophysiol. *97*, 4296–4309.

Logothetis, N.K., and Sheinberg, D.L. (1996). Visual object recognition. Annu. Rev. Neurosci. *19*, 577–621.

Nienborg, H., and Cumming, B.G. (2006). Macaque V2 neurons, but not V1 neurons, show choice-related activity. J. Neurosci. *26*, 9567–9578.

Nienborg, H., and Cumming, B.G. (2009). Decision-related activity in sensory neurons reflects more than a neuron's causal effect. Nature *459*, 89–92.

Parker, A.J. (2007). Binocular depth perception and the cerebral cortex. Nat. Rev. Neurosci. *8*, 379–391.

Philips, F., and Todd, J.T. (1996). Perception of local three-dimensional shape. J. Exp. Psychol. *22*, 930–944.

Preston, T.J., Li, S., Kourtzi, Z., and Welchman, A.E. (2008). Multivoxel pattern selectivity for perceptually relevant binocular disparities in the human brain. J. Neurosci. *28*, 11315–11327.

Riesenhuber, M., and Poggio, T. (1999). Hierarchical models of object recognition in cortex. Nat. Neurosci. *2*, 1019–1025.

Romo, R., Hernández, A., Zainos, A., and Salinas, E. (1998). Somatosensory discrimination based on cortical microstimulation. Nature *392*, 387–390.

Salzman, C.D., Britten, K.H., and Newsome, W.T. (1990). Cortical microstimulation influences perceptual judgements of motion direction. Nature *346*, 174–177.

Salzman, C.D., Murasugi, C.M., Britten, K.H., and Newsome, W.T. (1992). Microstimulation in visual area MT: effects on direction discrimination performance. J. Neurosci. *12*, 2331–2355.

Sáry, G., Vogels, R., and Orban, G.A. (1993). Cue-invariant shape selectivity of macaque inferior temporal neurons. Science *260*, 995–997.

Schwartz, E.L., Desimone, R., Albright, T.D., and Gross, C.G. (1983). Shape recognition and inferior temporal neurons. Proc. Natl. Acad. Sci. USA *80*, 5776–5778.

Srivastava, S., Orban, G.A., De Mazière, P.A., and Janssen, P. (2009). A distinct representation of three-dimensional shape in macaque anterior intraparietal area: fast, metric, and coarse. J. Neurosci. *29*, 10613–10626.

Tanaka, K. (1996). Inferotemporal cortex and object vision. Annu. Rev. Neurosci. *19*, 109–139.

Tehovnik, E.J., Tolias, A.S., Sultan, F., Slocum, W.M., and Logothetis, N.K. (2006). Direct and indirect activation of cortical neurons by electrical microstimulation. J. Neurophysiol. *96*, 512–521.

Thomas, E., Van Hulle, M.M., and Vogels, R. (2001). Encoding of categories by noncategory-specific neurons in the inferior temporal cortex. J. Cogn. Neurosci. *13*, 190–200.

Thomas, O.M., Cumming, B.G., and Parker, A.J. (2002). A specialization for relative disparity in V2. Nat. Neurosci. *5*, 472–478.

Tsutsui, K., Jiang, M., Yara, K., Sakata, H., and Taira, M. (2001). Integration of perspective and disparity cues in surface-orientation-selective neurons of area CIP. J. Neurophysiol. *86*, 2856–2867.

Uka, T., and DeAngelis, G.C. (2004). Contribution of area MT to stereoscopic depth perception: choice-related response modulations reflect task strategy. Neuron *42*, 297–310.

Uka, T., and DeAngelis, G.C. (2006). Linking neural representation to function in stereoscopic depth perception: roles of the middle temporal area in coarse versus fine disparity discrimination. J. Neurosci. *26*, 6791–6802.

Uka, T., Tanabe, S., Watanabe, M., and Fujita, I. (2005). Neural correlates of fine depth discrimination in monkey inferior temporal cortex. J. Neurosci. *25*, 10796–10802.

Umeda, K., Tanabe, S., and Fujita, I. (2007). Representation of stereoscopic depth based on relative disparity in macaque area V4. J. Neurophysiol. *98*, 241–252.

Verhoef, B.E., Vogels, R., and Janssen, P. (2010). Contribution of inferior temporal and posterior parietal activity to three-dimensional shape perception. Curr. Biol. *20*, 909–913.

Vogels, R. (1999). Categorization of complex visual images by rhesus monkeys. Part 2: single-cell study. Eur. J. Neurosci. *11*, 1239–1255.

Yamane, Y., Carlson, E.T., Bowman, K.C., Wang, Z., and Connor, C.E. (2008). A neural code for three-dimensional object shape in macaque inferotemporal cortex. Nat. Neurosci. *11*, 1352–1360.

Zhang, T., and Britten, K.H. (2011). Parietal area VIP causally influences heading perception during pursuit eye movements. J. Neurosci. *31*, 2569–2575.